JOURNAL OF VIROLOGY, Nov. 2002, p. 11113–11122 Vol. 76, No. 21
0022-538X/02/$04.00+0 DOI: 10.1128/JVI.76.21.11113–11122.2002

Differential Requirements for COPI Coats in Formation of Replication Complexes among Three Genera of *Picornaviridae*

Elena V. Gazina,[1,2]* Jason M. Mackenzie,[3] Rebecca J. Gorrell,[1]† and David A. Anderson[1]

Macfarlane Burnet Institute for Medical Research and Public Health, Melbourne, Victoria 3004,[1] and Sir Albert Sakzewski Virus Research Centre, Royal Children's Hospital, Herston, Queensland 4029,[3] Australia, and D. I. Ivanovsky Institute of Virology, Moscow 123098, Russia[2]

Received 19 February 2002/Accepted 22 July 2002

Picornavirus RNA replication requires the formation of replication complexes (RCs) consisting of virus-induced vesicles associated with viral nonstructural proteins and RNA. Brefeldin A (BFA) has been shown to strongly inhibit RNA replication of poliovirus but not of encephalomyocarditis virus (EMCV). Here, we demonstrate that the replication of parechovirus 1 (ParV1) is partly resistant to BFA, whereas echovirus 11 (EV11) replication is strongly inhibited. Since BFA inhibits COPI-dependent steps in endoplasmic reticulum (ER)-Golgi transport, we tested a hypothesis that different picornaviruses may have differential requirements for COPI in the formation of their RCs. Using immunofluorescence and cryo-immunoelectron microscopy we examined the association of a COPI component, β-COP, with the RCs of EMCV, ParV1, and EV11. EMCV RCs did not contain β-COP. In contrast, β-COP appeared to be specifically distributed to the RCs of EV11. In ParV1-infected cells β-COP was largely dispersed throughout the cytoplasm, with some being present in the RCs. These results suggest that there are differences in the involvement of COPI in the formation of the RCs of various picornaviruses, corresponding to their differential sensitivity to BFA. EMCV RCs are likely to be formed immediately after vesicle budding from the ER, prior to COPI association with membranes. ParV1 RCs are formed from COPI-containing membranes but COPI is unlikely to be directly involved in their formation, whereas formation of EV11 RCs appears to be dependent on COPI association with membranes.

All positive-stranded RNA viruses examined so far modify intracellular membranes of their host cells to create vesicular structures (replication complexes) in which viral RNA replication takes place. The replication complexes formed by viruses of different families have diverse morphology, and membranes of different cellular compartments undergo proliferation and reorganization in the process of their formation (6, 7, 11, 29, 38, 45).

The *Picornaviridae* are a family of positive-stranded RNA viruses, currently divided into nine genera (22). Most of the data on RNA replication of picornaviruses has been obtained in studies with *Poliovirus* (PV) (a member of the *Enterovirus* genus). The replication complexes isolated from PV-infected cells appear as rosette-like assemblies of heterogeneous-size vesicles associated with viral nonstructural proteins and RNA (3, 4). The exact origin of these vesicles is not clear. Rust et al. have demonstrated that early in PV infection, vesicles carrying viral nonstructural proteins are formed at the endoplasmic reticulum (ER) by the cellular COPII budding mechanism and thus are homologous to the vesicles of the anterograde membrane transport pathway (43). These findings are in contrast to some earlier studies, which suggested an autophagic mechanism for the formation of virus-induced vesicles from the ER (9, 46, 50). At later times in PV infection, when vesicle formation and RNA synthesis are at their peaks, all cytoplasmic membranes, except the nuclear and plasma membranes and mitochondria, are no longer recognizable (9). At this stage of infection, cellular protein markers of the ER, *trans*-Golgi, and lysosomes have been found within the PV-induced membranes (46).

Infection of cells with PV causes an inhibition of cellular protein secretion (13). Nevertheless, the virus appears to require some cellular components of the secretory pathway for RNA replication. Brefeldin A (BFA), an inhibitor of secretory membrane traffic in normal cells, strongly inhibits PV RNA synthesis in infected cells, but not viral entry, translation, or morphogenesis (21, 33, 52). This effect of BFA on PV replication is due to the inhibition of a required cellular factor, as PV replication in BFA-resistant cell lines is not affected (12).

In mammalian cells secretory membrane traffic between the ER and the Golgi is dependent on the function of two coat protein complexes, COPI and COPII. In the anterograde direction, ER cargo is packaged into COPII-coated vesicles that bud from the ER and fuse either with a preexisting vesicular-tubular cluster (VTC) (the functional equivalent of the intermediate compartment) or with each other to form a VTC de novo. In a second step, COPI binds to the VTC, and the COPI-coated VTC, containing no detectable amounts of COPII, travels to the Golgi complex (see reference 49 and references therein). COPI binding is required also for the retrieval of cycling proteins from the VTCs, the Golgi complex, and the *trans*-Golgi network, such retrograde-directed cargo probably being delivered to the ER in COPI-coated vesicles or uncoated tubules (23, 24, 27, 36). BFA prevents membrane binding of COPI and formation of COPI-coated vesicles by preventing the membrane association of the GTPase ARF1, which is a regulatory component of the COPI coat (14–17, 20, 37, 48).

* Corresponding author. Mailing address: Macfarlane Burnet Institute for Medical Research and Public Health, GPO Box 2284, Melbourne, Victoria 3001, Australia. Phone: 61 3 9282 2236. Fax: 61 3 9282 2100. E-mail: gazina@burnet.edu.au.

† Present address: Murdoch Children's Research Institute, Royal Children's Hospital, Parkville, Victoria 3052, Australia.

The formation of COPII-coated vesicles is not affected by BFA (1, 35, 47, 53).

Cuconati et al. have shown that inhibition of PV RNA replication by BFA in a cell-free system is due to a requirement for ARF activity for the formation of replication complexes (8). This would suggest that COPI may be essential for PV RNA replication. However, examination of two other picornaviruses, belonging to the *Rhinovirus* and *Cardiovirus* genera, has shown that while *Rhinovirus* replication is also inhibited by BFA, *Cardiovirus* replication is not affected (21). These results suggest that picornaviruses of different genera may require different cellular factors for RNA replication.

In this study, we demonstrate that the replication of *Parechovirus 1* (ParV1) (a member of the genus *Parechovirus*) is partly resistant to the effect of BFA, but to a lesser degree than that of *Encephalomyocarditis virus* (EMCV) (a member of the genus *Cardiovirus*), whereas replication of *Echovirus 11* (EV11) (a member of the genus *Enterovirus*) is strongly inhibited. Using cryo-immunoelectron microscopy (cryo-IEM) and confocal immunofluorescence (IF) microscopy we show that COPI-coated membranes are segregated from the replication complexes of EMCV, whereas ParV1 induces a diffusion of COPI throughout the cytoplasm, some of it being present in the replication complexes. In contrast, EV11 redistributes COPI to the sites of RNA replication. Our results suggest that COPI is directly involved in the formation of replication complexes of enteroviruses, but not cardioviruses or parechoviruses, which may explain the differences in BFA-sensitivity observed between the three genera of picornaviruses.

MATERIALS AND METHODS

Infections and BFA treatment. Monolayers of BS-C-1 cells (African green monkey kidney) were infected with EV11, ParV1, or EMCV at a multiplicity of infection (MOI) of 3 PFU per cell. The viruses were allowed to absorb for 1 h at 37°C in minimal essential medium (MEM) (Gibco) containing 1% fetal bovine serum (Gibco). The cells were then washed once with 10 mM Tris-HCl–150 mM NaCl (pH 7.5), and further incubated at 37°C in serum-free MEM, either containing BFA (10 μg/ml; Sigma) or not, for the indicated periods of time (calculated starting from the moment of virus addition to the cells).

Time course of viral RNA synthesis. BS-C-1 cells were infected with EV11, ParV1, or EMCV at an MOI of 3. After 1 h of virus absorption, the cells were washed and incubated in MEM containing [5,6-^{3}H]uridine (70 μCi/ml; Amersham). The cells were lysed at different times postinfection (p.i.), and total cytoplasmic RNA was extracted using an RNeasy kit (Qiagen) according to the instructions of the manufacturer. The RNA was electrophoresed through a formaldehyde–1% agarose gel and transferred to a Hybond-N membrane (Amersham) by capillary action in 1.5 M NaCl–150 mM sodium citrate (pH 7.0) for subsequent autoradiography.

Antibodies. Guinea pig polyclonal antibody raised against double-stranded RNA (dsRNA) was kindly provided by J.-Y. Lee (Victorian Infectious Diseases Reference Laboratory, Melbourne, Australia) (26). Monoclonal antibody to giantin was a gift of H.-P. Hauri (University of Basel, Basel, Switzerland) (28). Rabbit polyclonal antibody to β-COP was purchased from Affinity BioReagents.

Immunofluorescence. BS-C-1 cells on coverslips were infected as above and fixed with 4% paraformaldehyde in phosphate-buffered saline (PBS) for 10 min at 20°C, followed by permeabilization with 0.2% Triton X-100 in 4% paraformaldehyde for 10 min at 20°C. Double IF staining was performed using goat anti-guinea pig immunoglobulin G (IgG) antibody conjugated to Alexa Fluor 488 and goat anti-rabbit or anti-mouse IgG antibody conjugated to Alexa Fluor 568 (Molecular Probes). The images were obtained and processed using Radiance 2100 system for confocal microscopy (Bio-Rad).

Electron microscopy. For resin embedding, infected and uninfected cells were harvested in PBS and fixed with 3% glutaraldehyde in PBS. The samples were treated with 1% osmium tetroxide, dehydrated with ethanol, and embedded in Epon 612 resin as previously described (31). The protocol for cryo-IEM was described previously (30, 31). Briefly, cells were harvested in PBS and resuspended in 4% paraformaldehyde–0.2% glutaraldehyde in PBS. Cells were then washed in PBS and embedded in 10% gelatin before cryofixation. Ultrathin sections (50 nm) were collected in a 14:1 mix of 2.3 M sucrose and 2% methylcellulose and immunolabeled, using anti-IgG gold (Biocell) or protein A-gold (Utrecht University, Utrecht, Netherlands) for visualization. All specimens were examined on JEOL 1010 transmission electron microscope at 80 kV.

RESULTS

Parechovirus 1 replicates in the presence of BFA. To examine whether BFA resistance is a unique property of the cardioviruses within the *Picornaviridae* family, we compared the effect of BFA on the replication of EV11 (an *Enterovirus*), EMCV (a *Cardiovirus*), and ParV1 (a *Parechovirus*).

BS-C-1 cells were infected with each virus at an MOI of 3 and treated with 10-μg/ml BFA starting from 1 h p.i., or left untreated. Samples were collected at 1-h intervals, and virus production over time was measured by plaque assay. The results demonstrated a reduction of 5 orders of magnitude in EV11 yield in the presence of BFA (from 2.7×10^7 PFU/ml to 2.7×10^2 PFU/ml), whereas EMCV production remained unaffected (2.3×10^5 PFU/ml) (Fig. 1A and C). These results were consistent with previously published data on PV and EMCV (21, 33). ParV1 demonstrated resistance to BFA, however to a lower extent than EMCV: a 4-fold reduction in the virus yield was observed in the presence of BFA (from 2.4×10^7 PFU/ml to 6×10^6 PFU/ml) (Fig. 1B). BFA had no significant effect on the time course of EMCV and ParV1 replication: virus production started and stopped at the same time points in BFA-treated and untreated cells (Fig. 1B and C).

These results have shown that ParV1, like EMCV, is able to replicate in the presence of BFA, whereas EV11 replication, like PV replication, is strongly inhibited by BFA.

Effect of BFA on viral RNA synthesis. To compare the effect of BFA on RNA replication between the three viruses, we first selected the time points corresponding to the peak RNA synthesis for each virus. For that purpose, BS-C-1 cells were infected with each virus at an MOI of 3 and labeled with [5,6-^{3}H]uridine starting from 1 h p.i. Cytoplasmic RNA was extracted from the cells at different times p.i. and analyzed by formaldehyde-agarose gel electrophoresis and autoradiography. The time courses showed maximal activity of viral RNA synthesis between 5 and 6 h p.i for EV11, between 5 and 7 h p.i. for ParV1, and between 7 and 8 h p.i. for EMCV (Fig. 2), consistent with the time courses of virus production (Fig. 1). On this basis we selected the time points of 5.5, 6, and 7.5 h p.i for EV11, ParV1 and EMCV, respectively.

Next, we examined the RNA replication sites in the cells infected with EMCV, ParV1, and EV11 and treated with 10-μg/ml BFA starting from 1 h p.i., or left untreated. The cells were fixed at 7.5, 6, and 5.5 h p.i. for EMCV, ParV1, and EV11, respectively, and stained for IF using an antibody directed against dsRNA, which interacts with replicative forms of viral RNA (26, 29, 54).

In the absence of BFA, the cytoplasmic distribution of the RNA replication sites appeared to be similar between EMCV and EV11, with numerous small foci of anti-dsRNA staining concentrated in the perinuclear and juxtanuclear areas (Fig. 3A and E). In ParV1-infected cells the foci of anti-dsRNA staining were larger and fewer than those observed in EMCV- and EV11-infected cells; however, they were also concentrated

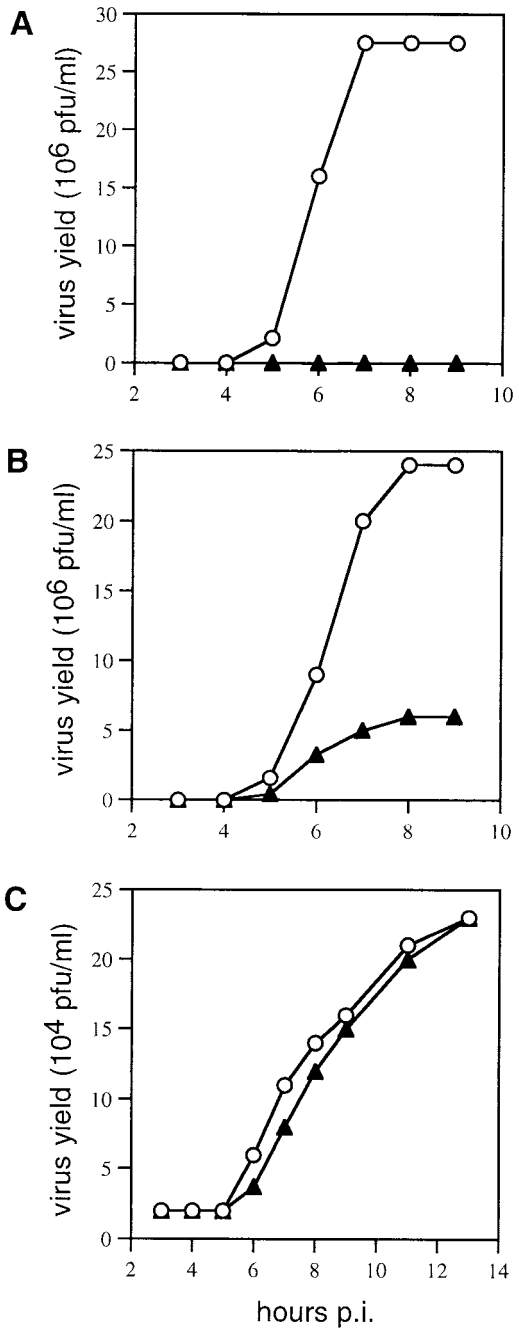

FIG. 1. Time course of EV11, ParV1, and EMCV production. BS-C-1 cells were infected with EV11 (A), ParV1 (B), or EMCV (C) at an MOI of 3 and treated with 10-μg/ml BFA starting from 1 h p.i. (▲) or left untreated (○). Cells were harvested into culture medium at indicated times, and virus yield was measured by plaque assay.

in the perinuclear and juxtanuclear areas (Fig. 3C). The pattern of EMCV dsRNA staining did not change in the presence of BFA (Fig. 3B). The pattern of ParV1 dsRNA staining also did not change, except for the reduction in the number of the foci (Fig. 3D), consistent with the reduction in the virus yield described above. In contrast, no dsRNA could be detected in EV11 samples (Fig. 3F), consistent with the profound inhibition of replication of this virus by BFA.

Morphology of the replication complexes of EMCV, ParV1, and EV11. As a first step towards defining the cellular factors involved in the formation of the replication complexes (RCs) of EMCV, ParV1 and EV11, we compared the morphology of the RCs between the three viruses.

First, we utilized resin embedding and electron microscopy of the cells infected for 7.5, 6 and 5.5 h with EMCV, ParV1 and EV11, respectively, in the absence of BFA. Thus, we observed that all three viruses induced a clustering of vesicles within the perinuclear region of the cytoplasm (Fig. 4A to C), consistent with previous reports for the viruses from the same genera (9, 19, 51). EMCV and EV11 induced similar assemblies of tightly clustered vesicles (Fig. 4A and C). The vesicles within the membranous structures induced by ParV1 were less tightly clustered (Fig. 4B). Cells infected with any of the three viruses appeared to contain neither visible Golgi bodies nor ordered rough ER, which were readily observed in mock-infected cells (data not shown).

To further examine possible structural differences between the RCs formed by the three viruses we used cryo-IEM, which allowed us to specifically visualize the RCs using the anti-dsRNA antibody and gold-labeled conjugate. We observed that in EMCV-infected cells, dsRNA was localized to electron-dense structures within the induced vesicle clusters (arrow in Fig. 4D). In EV11-infected cells dsRNA was localized to electron-dense structures within the vesicle clusters (arrows in Fig. 4F), similar to EMCV, but also to the membrane of the vesicles (arrowheads in Fig. 4F). The vesicles in both EMCV and EV11 RCs were heterogeneous in size and appeared to have a poorly defined outer membrane, possibly due to fusion with adjacent vesicles or due to some modification of the lipid composition.

In contrast, ParV1 RCs comprised well-defined, homogeneously sized vesicles approximately 70 to 100 nm in diameter and did not appear to contain the electron-dense structures observed with EMCV and EV11 (Fig. 4E). dsRNA was associated with the membrane of the induced vesicles.

Thus, the RCs of EMCV and EV11 appeared to have similar morphology, consisting of clusters of poorly defined, heterogeneously sized vesicles with electron-dense structures, whereas the ParV1 RCs were distinct, consisting of clusters of well defined homogeneous vesicles without electron-dense structures.

β-COP colocalizes with EV11, but not EMCV, dsRNA at the peak of RNA synthesis. Rust et al. have demonstrated that the vesicles in PV replication complexes are homologous to the vesicles of the anterograde membrane transport pathway (43). Assuming that the same is true for all picornaviruses, the basis of their differential sensitivity to BFA may reside in a stage of the ER-to-Golgi pathway, which these vesicles are required to reach for the formation of the RCs. Provided that budding of COPII-coated vesicles from the ER is not affected by BFA (1, 35, 47, 53), it is logical to presume that enteroviruses may require COPI-coated membranes, whereas cardio- and parechoviruses may use membranes at earlier stages of anterograde transport. To test this hypothesis we examined whether a component of COPI, β-COP, colocalized with dsRNA in EMCV-, EV11-, or ParV1-infected cells, using confocal IF microscopy and cryo-IEM.

By confocal IF microscopy we observed that the foci of anti-β-COP and anti-dsRNA staining in EMCV-infected cells

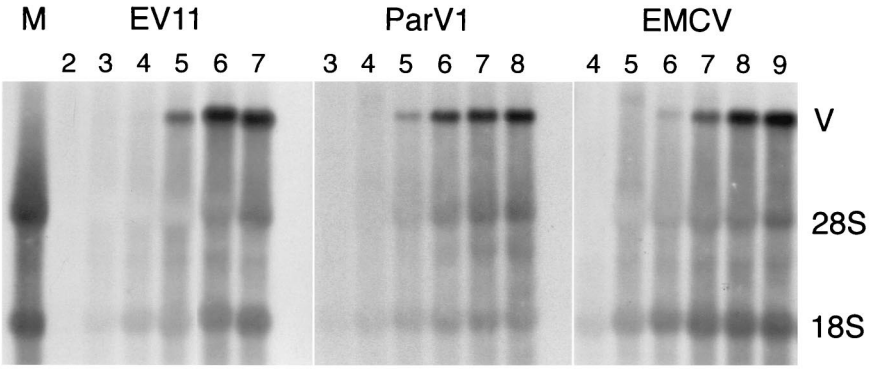

FIG. 2. Time course of EV11, ParV1, and EMCV RNA synthesis. BS-C-1 cells were infected with each virus at MOI of 3 and labeled with [5,6-^{3}H]uridine starting from 1 h p.i. Cytoplasmic RNA was extracted from the cells at indicated times (hours) after infection and analyzed by formaldehyde-agarose gel electrophoresis and autoradiography. The positions of viral (V) and cellular ribosomal (28S and 18S) RNAs are marked on the right. M, RNA extracted from mock-infected cells labeled with [5,6-^{3}H]uridine for 10 h.

did not colocalize, and indeed the distribution of the two markers was different: the areas of more intense anti-β-COP staining appeared to contain fewer anti-dsRNA foci (Fig. 5A to C). ParV1 infection resulted in a strong reduction in anti-β-COP staining, suggestive of dispersal of most COPI throughout the cytoplasm (Fig. 5D to F). The low intensity of anti-β-COP staining in ParV1-infected cells precluded observation of any possible colocalization with dsRNA by confocal IF microscopy.

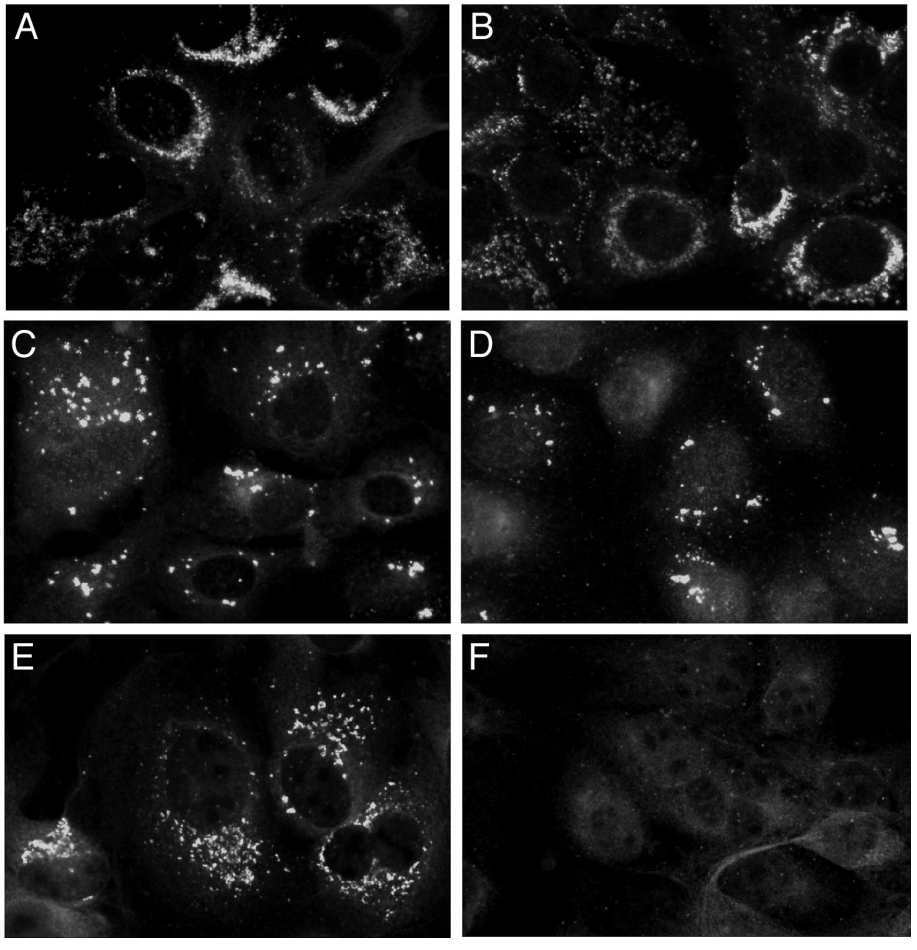

FIG. 3. Distribution of dsRNA in BS-C-1 cells infected with EMCV, ParV1, or EV11 in the absence or presence of BFA. Cells were infected with EMCV (A and B), ParV1 (C and D), or EV11 (E and F) at an MOI of 3 and treated with 10-μg/ml BFA starting from 1 h p.i. (B, D, and F) or left untreated (A, C, and E). The cells were fixed at 7.5, 6, and 5.5 h p.i. for EMCV, ParV1, and EV11, respectively, and immunostained with anti-dsRNA antibody and Alexa Fluor 488 conjugate.

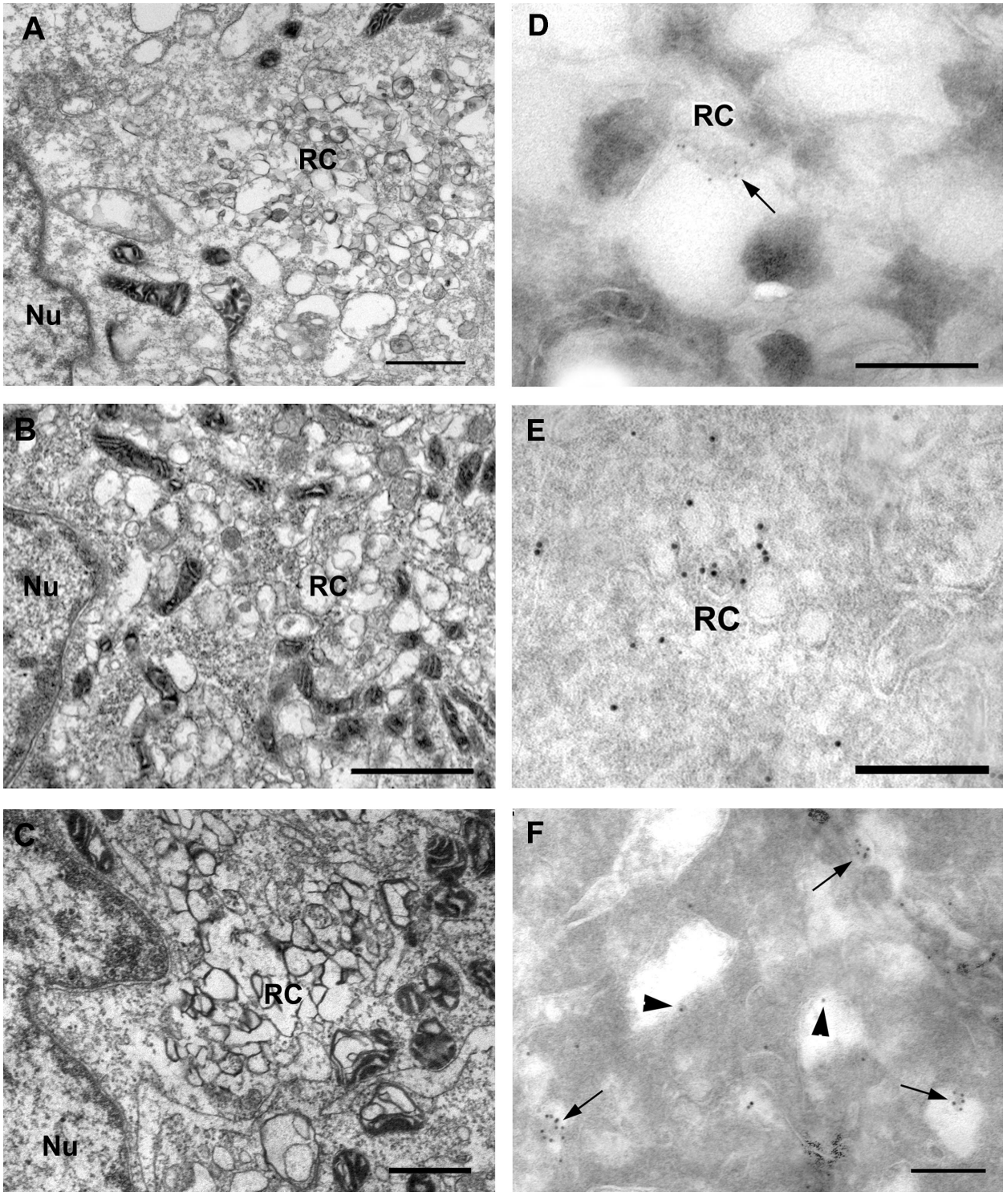

FIG. 4. Morphology of the replication complexes of EMCV, ParV1 and EV11. BS-C-1 cells were infected with EMCV (A and D), ParV1 (B and E), or EV11 (C and F) at an MOI of 3; incubated for 7.5, 6, or 5.5 h, respectively; and then harvested and fixed for electron microscopy. (A to C) Cells were embedded in Epon resin, and ultrathin sections were cut and stained with uranyl acetate and lead citrate. All viruses induced the clustering of vesicles in the perinuclear region indicative of picornavirus RCs. Nu, nucleus. Bars, 1 μm. (D to F) Ultrathin cryosections of infected cells were immunolabeled with anti-dsRNA antibody and visualized with either 5-nm anti-IgG gold (D) or 10-nm protein A-gold (E and F). (D) In EMCV-infected cells, labeling of dsRNA was localized to electron-dense structures (indicated by arrows) within the clusters of heterogeneous vesicles. (E) ParV1-infected cells were labeled on clusters of homogeneous vesicles ranging in size between 70 and 100 nm. The anti-dsRNA antibody appeared to specifically label the membrane of the vesicles. (F) EV11-infected cells displayed labeling of dsRNA within the clusters of heterogeneous vesicles, associated with electron-dense structures (indicated by arrows), as for EMCV, and also with the membrane of the vesicles (indicated by arrowheads). Bars, 200 nm.

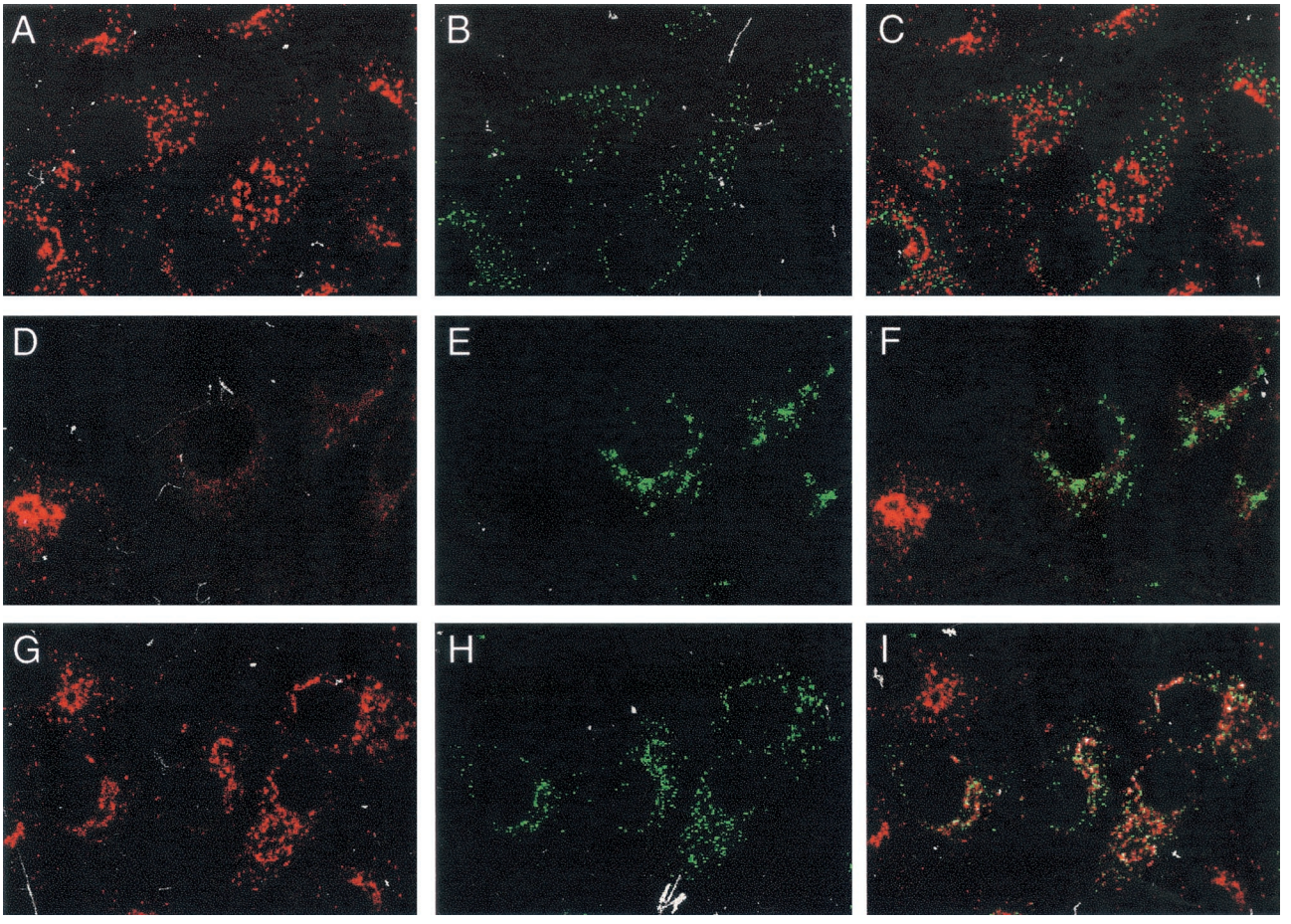

FIG. 5. The distribution of β-COP and dsRNA in cells infected with EMCV, ParV1, and EV11 visualized by confocal IF microscopy. Cells were infected as in Fig. 4, then fixed and double-labeled with anti-dsRNA and anti-β-COP antibodies. (A, D, and G) Staining with anti-β-COP antibody and Alexa Fluor 568 conjugate (red). (B, E, and H) Staining with anti-dsRNA antibody and Alexa Fluor 488 conjugate (green). (C, F, and I) Merge of first two columns; the sites of colocalization of the two antibodies are highlighted in yellow. (A to C) EMCV-infected cells; no colocalization. (D to F) ParV1-infected cells; strong reduction in anti-β-COP staining is obvious in comparison with an uninfected cell present in this sample. (G to I) EV11-infected cells; partial colocalization of the two antibodies.

In contrast, the patterns of anti-dsRNA and anti-β-COP staining in EV11-infected cells were very similar, and partial colocalization of the two antibodies was observed (Fig. 5G to I).

When the infected cells were further examined by cryo-IEM, the EMCV RCs did not contain β-COP (small arrowheads in Fig. 6A and B), although it was present on some vesicles in the vicinity (large arrowheads in Fig. 6A and B). In contrast, both ParV1 and EV11 RCs were colabeled with anti-dsRNA and anti-β-COP antibodies (Fig. 6C-F).

These results suggested that COPI-coated vesicles may be involved in the formation of replication complexes of EV11, but not EMCV. The data for ParV1 are less conclusive. It would appear that, like EV11, ParV1 also uses COPI-coated membranes for assembly of the RCs. However, in contrast to EV11, which appeared to redistribute COPI coats to the virus-induced vesicular structures, ParV1 infection caused the dispersal of most COPI.

β-COP colocalizes with EV11 dsRNA early in infection. A hallmark of PV infection is the breakdown of the Golgi apparatus soon after the start of formation of RCs (5). The *trans*-Golgi marker β-1,4-galactosyltransferase (GalT) has been found within PV-induced membranes isolated from infected cells late in infection (46), and it was suggested that Golgi membranes may be used as a secondary source of vesicles for RCs following Golgi apparatus disintegration (43). Taking this into account we examined whether β-COP colocalized with dsRNA in EV11-infected cells early in infection, prior to disintegration of the Golgi complex. EMCV- and ParV1-infected cells were also examined at early times p.i. for comparison.

Viral dsRNA is first detectable in the infected cells by IF at 4 h p.i. for EV11 and ParV1 and at 5 h p.i. for EMCV (data not shown). Therefore, we examined whether β-COP colocalized with dsRNA in the infected cells at 4 h p.i. for EV11 and ParV1, and at 5 h p.i. for EMCV, using confocal IF microscopy. The integrity of the Golgi complex was monitored in the same experiments by double labeling of separate samples with anti-dsRNA antibody and an antibody to a marker for the *cis*- and medial-Golgi compartments, giantin.

No colocalization between β-COP and dsRNA was observed in EMCV- and ParV1-infected cells: the staining patterns of β-COP and dsRNA in EMCV-infected cells were not coincident (Fig. 7A to C), and ParV1 caused strong reduction in

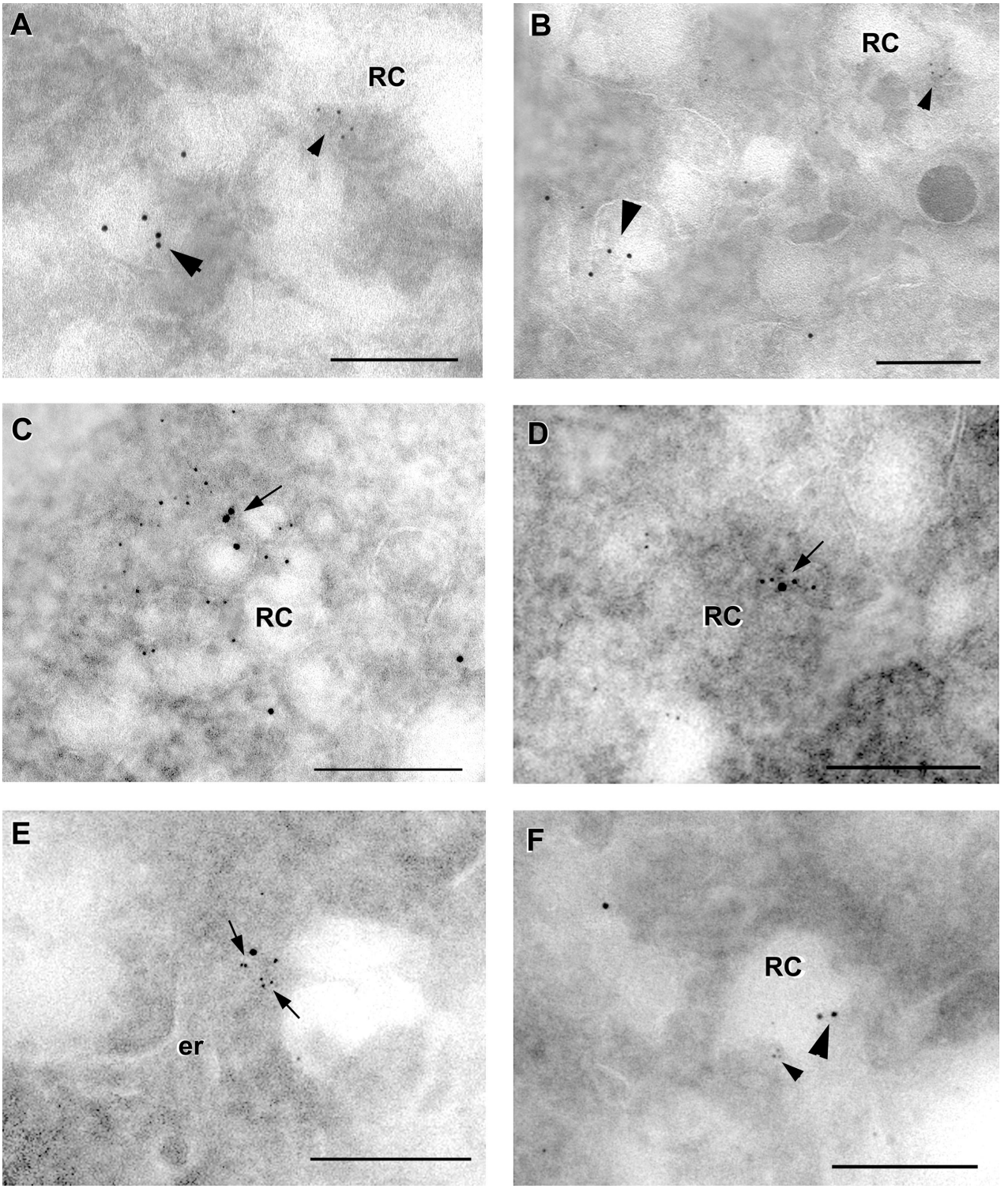

FIG. 6. β-COP is present within the RCs of ParV1 and EV11 but is absent from the RCs of EMCV. Cells were infected as in Fig. 4, then harvested, processed for cryosectioning, and double-immunolabeled with anti-dsRNA (5-nm gold conjugate) and anti-β-COP (10-nm gold conjugate) antibodies. In EMCV-infected cells (A and B) the two markers (large arrowheads indicating β-COP and small arrowheads indicating dsRNA) appeared distinct from each other. ParV1 (C and D)- and EV11 (E)-infected cells showed coincidental labeling as indicated by the arrows. In panel E, anti-β-COP and anti-dsRNA antibodies are bound to a vesicular structure budding from a membrane in close proximity to the ER. (F) Both anti-β-COP (large arrowhead) and anti-dsRNA (small arrowhead) antibodies within an EV11 RC, although not very close to each other. Bars, 200 nm.

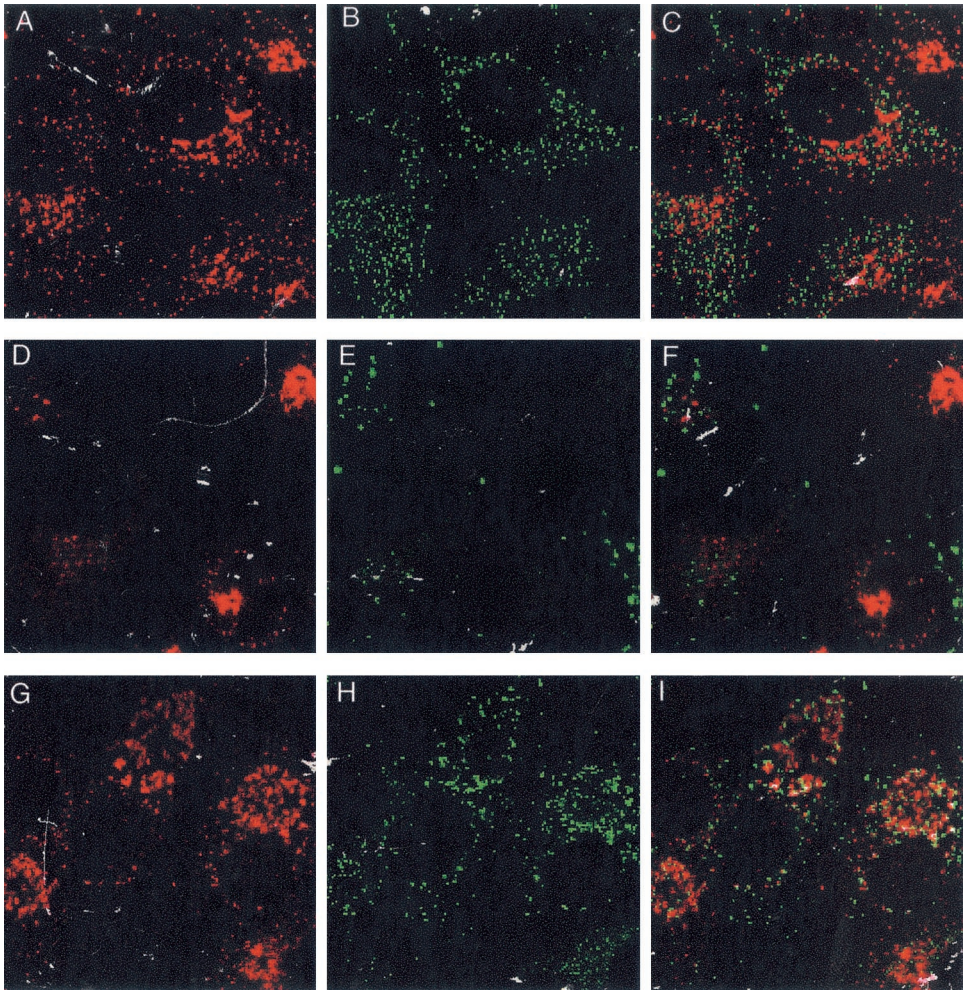

FIG. 7. Distribution of β-COP and dsRNA in the cells at early times in EMCV, ParV1, and EV11 infections. Cells were infected with EMCV (A to C), ParV1 (D to F), or EV11 (G to I) at an MOI of 3. The infected cells were fixed at 5 h p.i. (EMCV) or 4 h p.i. (ParV1 and EV11), double-labeled with anti-dsRNA and anti-β-COP antibodies, and visualized by confocal IF microscopy. (A, D, and G) Staining with anti-β-COP antibody and Alexa Fluor 568 conjugate (red). (B, E, and H) Staining with anti-dsRNA antibody and Alexa Fluor 488 conjugate (green). (C, F, and I) Merge of first two columns; the sites of colocalization of the two antibodies are highlighted in yellow.

β-COP staining (Fig. 7D to F). In contrast, β-COP partly colocalized with dsRNA in EV11-infected cells at 4 h p.i., although the extent of colocalization was lower than that observed at 5.5 h p.i. (compare Fig. 7I and 5I). The staining pattern of giantin in cells infected with EV11 for 4 h was similar to that in uninfected cells, suggesting that the Golgi complex was still intact (data not shown).

These results suggested that COPI-coated vesicles may be involved in the formation of the RCs of EV11 from the start of RNA replication.

DISCUSSION

BFA has been shown to strongly inhibit RNA replication of PV (an enterovirus) and a rhinovirus but to have no effect on the replication of the cardiovirus EMCV (21, 33). In this study, we have demonstrated that replication of the parechovirus ParV1 is also partially resistant to the effect of BFA, although not to the same extent as that of EMCV, whereas replication of another enterovirus, EV11, is strongly inhibited by BFA, like that of PV.

Replication complexes of EMCV and EV11 appeared to have similar morphologies when examined by cryo-IEM, consisting of clusters of heterogeneously sized, poorly defined vesicles, with dsRNA localized mainly to electron-dense structures within the clusters. Such electron-dense structures have previously been identified as the sites of PV RNA replication (2). Replication complexes of ParV1 were distinct, consisting of less tightly clustered, well-defined, homogeneous vesicles, not containing electron-dense structures. dsRNA was associated with the membrane of the vesicles.

Despite their morphological similarity, the RCs of EMCV and EV11 had a major difference in vesicle coating, which was consistent with the different sensitivity of these viruses to BFA.

A component of the COPI coat, β-COP, was observed within the RCs of EV11 by cryo-IEM, and confocal IF microscopy demonstrated that the staining patterns of β-COP and dsRNA were similar and partly colocalized both early and late

in EV11 infection, with the extent of colocalization being higher late in infection. Since COPI continuously binds to and dissociates from membranes with a half-life of less than 2 min (J. F. Presley, C. Miller, K. Zaal, J. Ellenberg, and J. Lippincott-Schwartz, abstr., Mol. Biol. Cell Suppl. **9:**746, 1998), the higher degree of association of COPI with EV11 RCs late in infection, after disruption of the Golgi complex, may be due to the increase in free cytoplasmic COPI caused by its release from disintegrated Golgi membranes.

These results suggest that COPI association with membranes may be required for the formation of the RCs of EV11 from the start of the replication cycle, a notion that can explain the profound inhibition by BFA of the replication of EV11. This hypothesis is supported by the previously published data that PV RNA replication in vitro is dependent on ARF activity (8).

It needs to be noted that in addition to COPI, BFA prevents association with membranes of another ARF1-regulated coat protein complex—clathrin-γ-adaptin (40, 41, 55)—thus preventing budding of clathrin-γ-adaptin-coated vesicles from the *trans*-Golgi network, endosomes, and lysosomes (10, 18). However, Doedens et al. have demonstrated that in cell lines in which COPI association with membranes is not affected by BFA, whereas clathrin-γ-adaptin association is inhibited, PV production is not affected by BFA (12). Therefore, clathrin-γ-adaptin-coated vesicles, even if present in the RCs of enteroviruses, have no significant role in their formation.

Another possible cause of the inhibition of replication of enteroviruses by BFA is Golgi complex disintegration and redistribution of Golgi lipids and enzymes into the ER, which is the consequence of COPI dissociation from membranes. However, the integrity of the Golgi complex does not appear to be important for the enterovirus RNA replication, since PV vesicles do not originate from nor fuse with the Golgi complex early in infection (43), and the Golgi complex disintegrates soon after the start of RNA synthesis (5). Redistribution of Golgi lipids and enzymes into the ER also seems unlikely to inhibit the formation of the RCs, because it does not affect budding of COPII-coated vesicles from the ER (35, 47, 53).

Thus, our results, in combination with the published data, strongly suggest that the formation of the RCs of enteroviruses is dependent on COPI association with the vesicles, and the inhibitory effect of BFA is due to prevention of such association.

Our findings are consistent with the data of Rust et al. that PV-induced vesicles bud from the ER by the COPII mechanism and therefore are homologous to the vesicles of the anterograde membrane transport pathway (43). We demonstrate that a later step in this pathway, COPI binding, is also required for the enterovirus RC formation. To the best of our knowledge, there are no published data suggesting an association of COPI with autophagy. Also, BFA does not interfere with the formation of autophagy (34, 39). Taken together, this argues against the autophagic mechanism for the formation of virus-induced vesicles on the ER (9, 46, 50).

It is not clear at what stage of the ER-Golgi pathway the RCs of enteroviruses are assembled. COPI coats are predominantly found on VTC and Golgi membranes and are found less so on the *trans*-Golgi network (reference 32 and references therein). Also, in vitro experiments have shown that COPI can be directly recruited to the vesicles after budding from the ER (42). It is possible, therefore, that ER-derived vesicles may acquire COPI coats prior to assembly into the RCs. Alternatively, ER-derived vesicles may fuse into VTCs, and a second, COPI-dependent budding step may be required for assembly of the RCs.

In contrast to EV11, EMCV RCs did not contain β-COP, as visualized by cryo-IEM, and confocal IF microscopy demonstrated segregation of the foci of staining of β-COP and dsRNA in EMCV-infected cells. Segregation of COPI from the replication complexes of EMCV was consistent with the observed resistance of EMCV to BFA.

These results suggest that RCs of EMCV are likely to be formed immediately after vesicle budding from the ER, without recruiting COPI coats. Budding of COPII-coated vesicles from the ER is not affected by BFA (1, 35, 47, 53), which can explain the insensitivity of EMCV replication to BFA.

ParV1 was distinct from EV11 and EMCV not only in the morphology of the RCs but also in its effect on COPI association with membranes. IF microscopy showed a strong reduction in β-COP staining in ParV1-infected cells, starting from early in infection, suggesting the dissociation of most COPI from the membranes and dispersal throughout the cytoplasm. Nevertheless, β-COP could be detected within the ParV1 RCs by cryo-IEM. These observations may mean that ParV1 RCs are formed using COPI-containing membranes, but their formation causes predominant dissociation of COPI rather than its involvement in RC formation. This would be consistent with the relative resistance of ParV1 to the effect of BFA. VTCs might be the source of such membranes. They normally contain COPI, and their formation is enhanced by COPI binding (25), but they still can form when COPI binding is inhibited (44, 53). The fourfold reduction in ParV1 yield in the presence of BFA might reflect a corresponding reduction in VTC formation. However, further studies are needed to test this hypothesis.

ACKNOWLEDGMENTS

This work was supported in part by NHMRC fellowship 149502 and project grant 149501 (D.A.A.) and by the Joe White Bequest and the Research Fund of the Burnet Institute (E.V.G.).

We thank J.-Y. Lee and H.-P. Hauri for generously providing the antibodies and J. Mak and R. Ghildyal for critical reading of the manuscript.

REFERENCES

1. **Bednarek, S. Y., M. Ravazzola, M. Hosobuchi, M. Amherdt, A. Perrelet, R. Schekman, and L. Orci.** 1995. COPI- and COPII-coated vesicles bud directly from the endoplasmic reticulum in yeast. Cell **83:**1183–1196.
2. **Bienz, K., D. Egger, and L. Pasamontes.** 1987. Association of polioviral proteins of the P2 genomic region with the viral replication complex and virus-induced membrane synthesis as visualized by electron microscopic immunocytochemistry and autoradiography. Virology **160:**220–226.
3. **Bienz, K., D. Egger, T. Pfister, and M. Troxler.** 1992. Structural and functional characterization of the poliovirus replication complex. J. Virol. **66:** 2740–2747.
4. **Bienz, K., D. Egger, M. Troxler, and L. Pasamontes.** 1990. Structural organization of poliovirus RNA replication is mediated by viral proteins of the P2 genomic region. J. Virol. **64:**1156–1163.
5. **Bolten, R., D. Egger, R. Gosert, G. Schaub, L. Landmann, and K. Bienz.** 1998. Intracellular localization of poliovirus plus- and minus-strand RNA visualized by strand-specific fluorescent in situ hybridization. J. Virol. **72:** 8578–8585.
6. **Burgyan, J., L. Rubino, and M. Russo.** 1996. The 5′-terminal region of a tombusvirus genome determines the origin of multivesicular bodies. J. Gen. Virol. **77:**1967–1974.

7. **Carette, J. E., M. Stuiver, J. Van Lent, J. Wellink, and A. Van Kammen.** 2000. Cowpea mosaic virus infection induces a massive proliferation of endoplasmic reticulum but not Golgi membranes and is dependent on de novo membrane synthesis. J. Virol. **74:**6556–6563.
8. **Cuconati, A., A. Molla, and E. Wimmer.** 1998. Brefeldin A inhibits cell-free, de novo synthesis of poliovirus. J. Virol. **72:**6456–6464.
9. **Dales, S., H. J. Eggers, I. Tamm, and G. E. Palade.** 1965. Electron microscopic study of the formation of poliovirus. Virology **26:**379–389.
10. **De Lisle, R. C., and R. Bansal.** 1996. Brefeldin A inhibits the constitutive-like secretion of a sulfated protein in pancreatic acinar cells. Eur. J. Cell Biol. **71:**62–71.
11. **De Zoeten, G. A., G. Gaard, and F. B. Diez.** 1972. Nuclear vesiculation associated with pea enation mosaic virus-infected plant tissue. Virology **48:**638–647.
12. **Doedens, J., L. A. Maynell, M. W. Klymkowsky, and K. Kirkegaard.** 1994. Secretory pathway function, but not cytoskeletal integrity, is required in poliovirus infection. Arch. Virol. Suppl. **9:**159–172.
13. **Doedens, J. R., and K. Kirkegaard.** 1995. Inhibition of cellular protein secretion by poliovirus proteins 2B and 3A. EMBO J. **14:**894–907.
14. **Donaldson, J. G., D. Finazzi, and R. D. Klausner.** 1992. Brefeldin A inhibits Golgi membrane-catalysed exchange of guanine nucleotide onto ARF protein. Nature **360:**350–352.
15. **Donaldson, J. G., R. A. Kahn, J. Lippincott-Schwartz, and R. D. Klausner.** 1991. Binding of ARF and beta-COP to Golgi membranes: possible regulation by a trimeric G protein. Science **254:**1197–1199.
16. **Donaldson, J. G., J. Lippincott-Schwartz, G. S. Bloom, T. E. Kreis, and R. D. Klausner.** 1990. Dissociation of a 110-kD peripheral membrane protein from the Golgi apparatus is an early event in brefeldin A action. J. Cell Biol. **111:**2295–2306.
17. **Donaldson, J. G., J. Lippincott-Schwartz, and R. D. Klausner.** 1991. Guanine nucleotides modulate the effects of brefeldin A in semipermeable cells: regulation of the association of a 110-kD peripheral membrane protein with the Golgi apparatus. J. Cell Biol. **112:**579–588.
18. **Fernandez, C. J., M. Haugwitz, B. Eaton, and H. P. Moore.** 1997. Distinct molecular events during secretory granule biogenesis revealed by sensitivities to brefeldin A. Mol. Biol. Cell **8:**2171–2185.
19. **Harb, J. M., and G. E. Burch.** 1973. Ultrastructural cytopathology of mouse myocardium associated with EMC viral infection. J. Mol. Cell Cardiol. **5:**55–62.
20. **Helms, J. B., and J. E. Rothman.** 1992. Inhibition by brefeldin A of a Golgi membrane enzyme that catalyses exchange of guanine nucleotide bound to ARF. Nature **360:**352–354.
21. **Irurzun, A., L. Perez, and L. Carrasco.** 1992. Involvement of membrane traffic in the replication of poliovirus genomes: effects of brefeldin A. Virology **191:**166–175.
22. **King, A. M. Q., F. Brown, P. D. Christian, T. Hovi, T. Hyypia, N. J. Knowles, S. M. Lemon, P. D. Minor, A. C. Palmenberg, T. Skern, and G. Stanway.** 2000. Picornaviridae, p. 657–673. *In* M. H. V. van Regenmortel, C. M. Fauquet, D. H. L. Bishop, C. H. Calisher, E. B. Carsten, M. K. Estes, S. M. Lemon, J. Maniloff, M. A. Mayo, D. McGeoch, C. R. Pringle, and R. B. Wickner (ed.), Virus taxonomy: classification and nomenclature of viruses. Seventh report of the International Committee for the Taxonomy of Viruses. Academic Press, San Diego, Calif.
23. **Klumperman, J., A. Schweizer, H. Clausen, B. L. Tang, W. Hong, V. Oorschot, and H. P. Hauri.** 1998. The recycling pathway of protein ERGIC-53 and dynamics of the ER-Golgi intermediate compartment. J. Cell Sci. **111:**3411–3425.
24. **Lanoix, J., J. Ouwendijk, C. C. Lin, A. Stark, H. D. Love, J. Ostermann, and T. Nilsson.** 1999. GTP hydrolysis by arf-1 mediates sorting and concentration of Golgi resident enzymes into functional COP I vesicles. EMBO J. **18:**4935–4948.
25. **Lavoie, C., J. Paiement, M. Dominguez, L. Roy, S. Dahan, J. N. Gushue, and J. J. Bergeron.** 1999. Roles for alpha(2)p24 and COPI in endoplasmic reticulum cargo exit site formation. J. Cell Biol. **146:**285–299.
26. **Lee, J. Y., J. A. Marshall, and D. S. Bowden.** 1994. Characterization of rubella virus replication complexes using antibodies to double-stranded RNA. Virology **200:**307–312.
27. **Letourneur, F., E. C. Gaynor, S. Hennecke, C. Demolliere, R. Duden, S. D. Emr, H. Riezman, and P. Cosson.** 1994. Coatomer is essential for retrieval of dilysine-tagged proteins to the endoplasmic reticulum. Cell **79:**1199–1207.
28. **Linstedt, A. D., M. Foguet, M. Renz, H. P. Seelig, B. S. Glick, and H. P. Hauri.** 1995. A C-terminally anchored Golgi protein is inserted into the endoplasmic reticulum and then transported to the Golgi apparatus. Proc. Natl. Acad. Sci. USA **92:**5102–5105.
29. **Mackenzie, J. M., M. K. Jones, and E. G. Westaway.** 1999. Markers for trans-Golgi membranes and the intermediate compartment localize to induced membranes with distinct replication functions in flavivirus-infected cells. J. Virol. **73:**9555–9567.
30. **Mackenzie, J. M., M. K. Jones, and P. R. Young.** 1996. Immunolocalization of the dengue virus nonstructural glycoprotein NS1 suggests a role in viral RNA replication. Virology **220:**232–240.
31. **Mackenzie, J. M., M. K. Jones, and P. R. Young.** 1996. Improved membrane preservation of flavivirus-infected cells with cryosectioning. J. Virol. Methods **56:**67–75.
32. **Martinez-Menarguez, J. A., H. J. Geuze, J. W. Slot, and J. Klumperman.** 1999. Vesicular tubular clusters between the ER and Golgi mediate concentration of soluble secretory proteins by exclusion from COPI-coated vesicles. Cell **98:**81–90.
33. **Maynell, L. A., K. Kirkegaard, and M. W. Klymkowsky.** 1992. Inhibition of poliovirus RNA synthesis by brefeldin A. J. Virol. **66:**1985–1994.
34. **Ogier-Denis, E., C. Bauvy, J. J. Houri, and P. Codogno.** 1997. Evidence for a dual control of macroautophagic sequestration and intracellular trafficking of N-linked glycoproteins by the trimeric G(i3) protein in HT-29 cells. Biochem. Biophys. Res. Commun. **235:**166–170.
35. **Orci, L., A. Perrelet, M. Ravazzola, F. T. Wieland, R. Schekman, and J. E. Rothman.** 1993. "BFA bodies": a subcompartment of the endoplasmic reticulum. Proc. Natl. Acad. Sci. USA **90:**11089–11093.
36. **Orci, L., M. Stamnes, M. Ravazzola, M. Amherdt, A. Perrelet, T. H. Sollner, and J. E. Rothman.** 1997. Bidirectional transport by distinct populations of COPI-coated vesicles. Cell **90:**335–349.
37. **Orci, L., M. Tagaya, M. Amherdt, A. Perrelet, J. G. Donaldson, J. Lippincott-Schwartz, R. D. Klausner, and J. E. Rothman.** 1991. Brefeldin A, a drug that blocks secretion, prevents the assembly of non-clathrin-coated buds on Golgi cisternae. Cell **64:**1183–1195.
38. **Pedersen, K. W., Y. van der Meer, N. Roos, and E. J. Snijder.** 1999. Open reading frame 1a-encoded subunits of the arterivirus replicase induce endoplasmic reticulum-derived double-membrane vesicles which carry the viral replication complex. J. Virol. **73:**2016–2026.
39. **Purhonen, P., K. Pursiainen, and H. Reunanen.** 1997. Effects of brefeldin A on autophagy in cultured rat fibroblasts. Eur. J. Cell Biol. **74:**63–67.
40. **Robinson, M. S.** 1990. Cloning and expression of gamma-adaptin, a component of clathrin-coated vesicles associated with the Golgi apparatus. J. Cell Biol. **111:**2319–2326.
41. **Robinson, M. S., and T. E. Kreis.** 1992. Recruitment of coat proteins onto Golgi membranes in intact and permeabilized cells: effects of brefeldin A and G protein activators. Cell **69:**129–138.
42. **Rowe, T., M. Aridor, J. M. McCaffery, H. Plutner, C. Nuoffer, and W. E. Balch.** 1996. COPII vesicles derived from mammalian endoplasmic reticulum microsomes recruit COPI. J. Cell Biol. **135:**895–911.
43. **Rust, R. C., L. Landmann, R. Gosert, B. L. Tang, W. Hong, H. P. Hauri, D. Egger, and K. Bienz.** 2001. Cellular COPII proteins are involved in production of the vesicles that form the poliovirus replication complex. J. Virol. **75:**9808–9818.
44. **Scales, S. J., R. Pepperkok, and T. E. Kreis.** 1997. Visualization of ER-to-Golgi transport in living cells reveals a sequential mode of action for COPII and COPI. Cell **90:**1137–1148.
45. **Schaad, M. C., P. E. Jensen, and J. C. Carrington.** 1997. Formation of plant RNA virus replication complexes on membranes: role of an endoplasmic reticulum-targeted viral protein. EMBO J. **16:**4049–4059.
46. **Schlegel, A., T. H. Giddings, Jr., M. S. Ladinsky, and K. Kirkegaard.** 1996. Cellular origin and ultrastructure of membranes induced during poliovirus infection. J. Virol. **70:**6576–6588.
47. **Shaywitz, D. A., L. Orci, M. Ravazzola, A. Swaroop, and C. A. Kaiser.** 1995. Human SEC13Rp functions in yeast and is located on transport vesicles budding from the endoplasmic reticulum. J. Cell Biol. **128:**769–777.
48. **Stamnes, M. A., and J. E. Rothman.** 1993. The binding of AP-1 clathrin adaptor particles to Golgi membranes requires ADP-ribosylation factor, a small GTP-binding protein. Cell **73:**999–1005.
49. **Stephens, D. J., N. Lin-Marq, A. Pagano, R. Pepperkok, and J. P. Paccaud.** 2000. COPI-coated ER-to-Golgi transport complexes segregate from COPII in close proximity to ER exit sites. J. Cell Sci. **113:**2177–2185.
50. **Suhy, D. A., T. H. Giddings, Jr., and K. Kirkegaard.** 2000. Remodeling the endoplasmic reticulum by poliovirus infection and by individual viral proteins: an autophagy-like origin for virus-induced vesicles. J. Virol. **74:**8953–8965.
51. **Trant, C. M., and R. M. Jamison.** 1975. Electron microscopic study of the morphogenesis of echovirus 23. Exp. Mol. Pathol. **22:**55–64.
52. **Tucker, S. P., C. L. Thornton, E. Wimmer, and R. W. Compans.** 1993. Vectorial release of poliovirus from polarized human intestinal epithelial cells. J. Virol. **67:**4274–4282.
53. **Ward, T. H., R. S. Polishchuk, S. Caplan, K. Hirschberg, and J. Lippincott-Schwartz.** 2001. Maintenance of Golgi structure and function depends on the integrity of ER export. J. Cell Biol. **155:**557–570.
54. **Westaway, E. G., J. M. Mackenzie, M. T. Kenney, M. K. Jones, and A. A. Khromykh.** 1997. Ultrastructure of Kunjin virus-infected cells: colocalization of NS1 and NS3 with double-stranded RNA, and of NS2B with NS3, in virus-induced membrane structures. J. Virol. **71:**6650–6661.
55. **Wong, D. H., and F. M. Brodsky.** 1992. 100-kD proteins of Golgi- and trans-Golgi network-associated coated vesicles have related but distinct membrane binding properties. J. Cell Biol. **117:**1171–1179.